Deep Learning for Remote Sensing Applications

He & Yokoya (2018): "Multi-Temporal Sentinel-1 and -2 Data Fusion for Optical Image Simulation", *ISPRS Int J Geo-Inf*, 7, 389, doi: 10.3390/ijgi7100389.

Christian Werner
chr.werner@me.com @cwerner76

TWiML & AI Meetup EMEA, 03.01.2019

remote sensing
IMPACT FACTOR 3.406
an Open Access Journal by MDPI

Deep Learning for Remote Sensing

Guest Editors:

Prof. Giovanni Poggi
Department of Electrical Engineering and Information Technology (DIETI), University Federico II of Naples (I), Via Claudio 21, 80125 Napoli, ITALY
poggi@unina.it

Dr. Giuseppe Scarpa
University Federico II of Naples, ITALY, Via Claudio 21, 80125 Naples, ITALY
giscarpa@unina.it

Dr. Luisa Verdoliva
University Federico II of Naples, ITALY, Via Claudio 21, 80125 Naples, ITALY
verdoliv@unina.it

Deadline for manuscript submissions:
closed (30 November 2018)

Message from the Guest Editors

Dear Colleagues,

This Special Issue aims to report the latest advances and trends concerning the application of deep learning to remote sensing problems. Papers of both theoretical and applicative nature are welcome, as well as contributions regarding new deep learning-oriented public datasets for the RS research community.

Major topics of interest, by no means exclusive, are:

- Large-scale datasets for training and testing deep learning solutions to RS problems;
- Deep learning for RS image processing (e.g., compression, denoising, segmentation, classification)
- Deep learning for RS image understanding (e.g., semantic labeling, object detection, data mining, image retrieval)
- Deep learning for RS data fusion (e.g., optical-SAR fusion, pan-sharpening)
- Deep learning with scarce or low-quality RS data, transfer learning, cross-sensor learning
- Processing of RS time-series through deep recurrent networks

Prof. Giovanni Poggi
Dr. Giuseppe Scarpa
Dr. Luisa Verdoliva
Guest Editors

mdpi.com/si/12002

Special Issue

Article
Mining Hard Negative Samples for SAR-Optical Image Matching Using Generative Adversarial Networks

Lloyd Haydn Hughes [1], Michael Schmitt [1] and Xiao Xiang Zhu [1,2,*]

Article
3D Façade Labeling over Complex Scenarios: A Case Study Using Convolutional Neural Network and Structure-From-Motion

Rodolfo Georjute Lotte [1,*], Norbert Haala [2], Mateusz Karpina [3], Luiz Eduardo Oliveira e Cruz de Aragão [1,4] and Yosio Edemir Shimabukuro [1]

Article
Geospatial Object Detection in Remote Sensing Imagery Based on Multiscale Single-Shot Detector with Activated Semantics

Shiqi Chen, Ronghui Zhan * and Jun Zhang

Article
CraterIDNet: An End-to-End Fully Convolutional Neural Network for Crater Detection and Identification in Remotely Sensed Planetary Images

Hao Wang, Jie Jiang * and Guangjun Zhang

Article
A Ship Rotation Detection Model in Remote Sensing Images Based on Feature Fusion Pyramid Network and Deep Reinforcement Learning

Kun Fu [1,2], Yang Li [1,2,*], Hao Sun [1], Xue Yang [1,2], Guangluan Xu [1,2], Yuting Li [3] and Xian Sun [1,2]

Article
Double Weight-Based SAR and Infrared Sensor Fusion for Automatic Ground Target Recognition with Deep Learning

Sungho Kim [1,*], Woo-Jin Song [2] and So-Hyun Kim [3]

Article
Automatic Ship Detection in Remote Sensing Images from Google Earth of Complex Scenes Based on Multiscale Rotation Dense Feature Pyramid Networks

Xue Yang [1,2], Hao Sun [1], Kun Fu [1,2,*], Jirui Yang [1,2], Xian Sun [1], Menglong Yan [1] and Zhi Guo [1]

Article
Building Extraction in Very High Resolution Remote Sensing Imagery Using Deep Learning and Guided Filters

Yongyang Xu [1], Liang Wu [1,2], Zhong Xie [1,2,*] and Zhanlong Chen [1]

Article
Siamese-GAN: Learning Invariant Representations for Aerial Vehicle Image Categorization

Laila Bashmal [1], Yakoub Bazi [1,*], Haikel AlHichri [1], Mohamad M. AlRahhal [2], Nassim Ammour [1] and Naif Alajlan [1]

Article
Long-Term Annual Mapping of Four Cities on Different Continents by Applying a Deep Information Learning Method to Landsat Data

Haobo Lyu [1,†], Hui Lu [1,2,*], Lichao Mou [3,4,†], Wenyu Li [1], Jonathon Wright [1,2], Xuecao Li [5], Xinlu Li [1,6], Xiao Xiang Zhu [3,4], Jie Wang [7], Le Yu [1,2] and Peng Gong [1,2]

Article
Improving Remote Sensing Scene Classification by Integrating Global-Context and Local-Object Features

Dan Zeng [1], Shuaijun Chen [1], Boyang Chen [2,*] and Shuying Li [3]

Article
Land Cover Segmentation of Airborne LiDAR Data Using Stochastic Atrous Network

Hasan Asy'ari Arief [1,*], Geir-Harald Strand [1,2], Håvard Tveite [1] and Ulf Geir Indahl [1]

Article
Deriving High Spatiotemporal Remote Sensing Images Using Deep Convolutional Network

Zhenyu Tan [1,2], Peng Yue [3,4,5,*], Liping Di [2,*] and Junmei Tang [2]

Article
Fast Cloud Segmentation Using Convolutional Neural Networks

Johannes Drönner [1,*], Nikolaus Korfhage [1], Sebastian Egli [2], Markus Mühling [1], Boris Thies [2], Jörg Bendix [2], Bernd Freisleben [1] and Bernhard Seeger [1]

Article
WeedMap: A Large-Scale Semantic Weed Mapping Framework Using Aerial Multispectral Imaging and Deep Neural Network for Precision Farming

Inkyu Sa [1,*,†], Marija Popović [1], Raghav Khanna [1], Zetao Chen [2], Philipp Lottes [3], Frank Liebisch [4], Juan Nieto [1], Cyrill Stachniss [3], Achim Walter [4] and Roland Siegwart [1]

Article
A CNN-Based Fusion Method for Feature Extraction from Sentinel Data

Giuseppe Scarpa [1,*], Massimiliano Gargiulo [1], Antonio Mazza [1] and Raffaele Gaetano [2,3]

Article
Scene Classification Based on a Deep Random-Scale Stretched Convolutional Neural Network

Yanfei Liu, Yanfei Zhong *, Feng Fei, Qiqi Zhu and Qianqing Qin

Article
Automatic Building Segmentation of Aerial Imagery Using Multi-Constraint Fully Convolutional Networks

Guangming Wu [1], Xiaowei Shao [1], Zhiling Guo [1], Qi Chen [1,2,*], Wei Yuan [1], Xiaodan Shi [1], Yongwei Xu [1] and Ryosuke Shibasaki [1]

Article
A Hierarchical Fully Convolutional Network Integrated with Sparse and Low-Rank Subspace Representations for PolSAR Imagery Classification

Yan Wang [1], Chu He [1,2,*], Xinlong Liu [1] and Mingsheng Liao [2,3]

Article
A Deep-Local-Global Feature Fusion Framework for High Spatial Resolution Imagery Scene Classification

Qiqi Zhu, Yanfei Zhong *, Yanfei Liu *, Liangpei Zhang and Deren Li

Article
Performance Evaluation of Single-Label and Multi-Label Remote Sensing Image Retrieval Using a Dense Labeling Dataset

Zhenfeng Shao, Ke Yang and Weixun Zhou *

Article
A Benchmark Dataset for Performance Evaluation of Multi-Label Remote Sensing Image Retrieval

Zhenfeng Shao, Ke Yang and Weixun Zhou *

Article
Dialectical GAN for SAR Image Translation: From Sentinel-1 to TerraSAR-X

Dongyang Ao [1,2], Corneliu Octavian Dumitru [1], Gottfried Schwarz [1] and Mihai Datcu [1,*]

Article
A Fast Dense Spectral–Spatial Convolution Network Framework for Hyperspectral Images Classification

Wenju Wang, Shuguang Dou *, Zhongmin Jiang and Liujie Sun

Article
Aircraft Type Recognition in Remote Sensing Images Based on Feature Learning with Conditional Generative Adversarial Networks

Yuhang Zhang [1,2], Hao Sun [1], Jiawei Zuo [1,2], Hongqi Wang [1], Guangluan Xu [1,2]

Article
Neural Network Based Kalman Filters for the Spatio-Temporal Interpolation of Satellite-Derived Sea Surface Temperature

Said Ouala [1,*], Ronan Fablet [1], Cédric Herzet [1,2], Bertrand Chapron [3], Ananda Pascual [4], Fabrice Collard [5] and Lucile Gaultier [5]

Sentinels Satellites

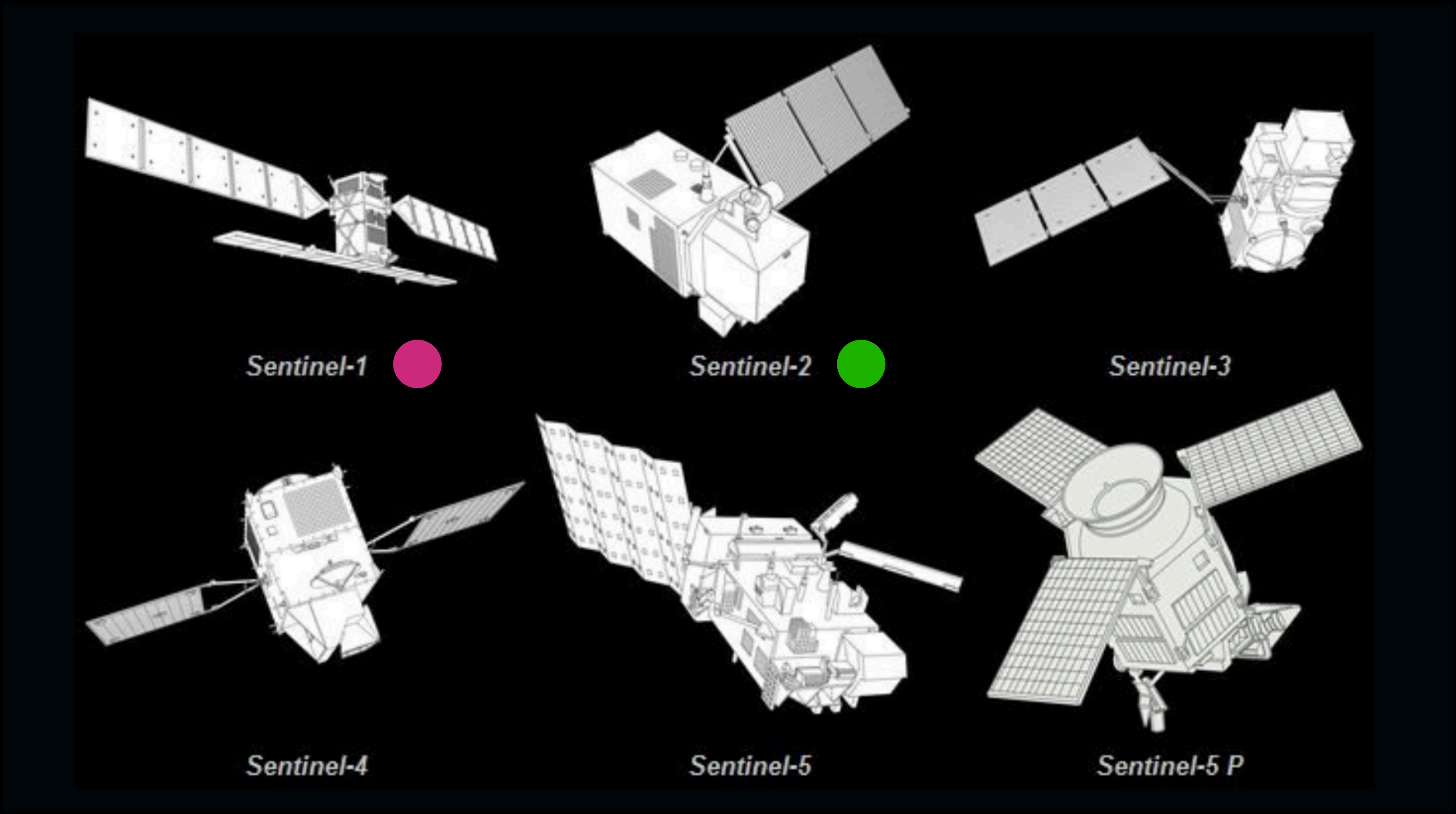

Source: ESA

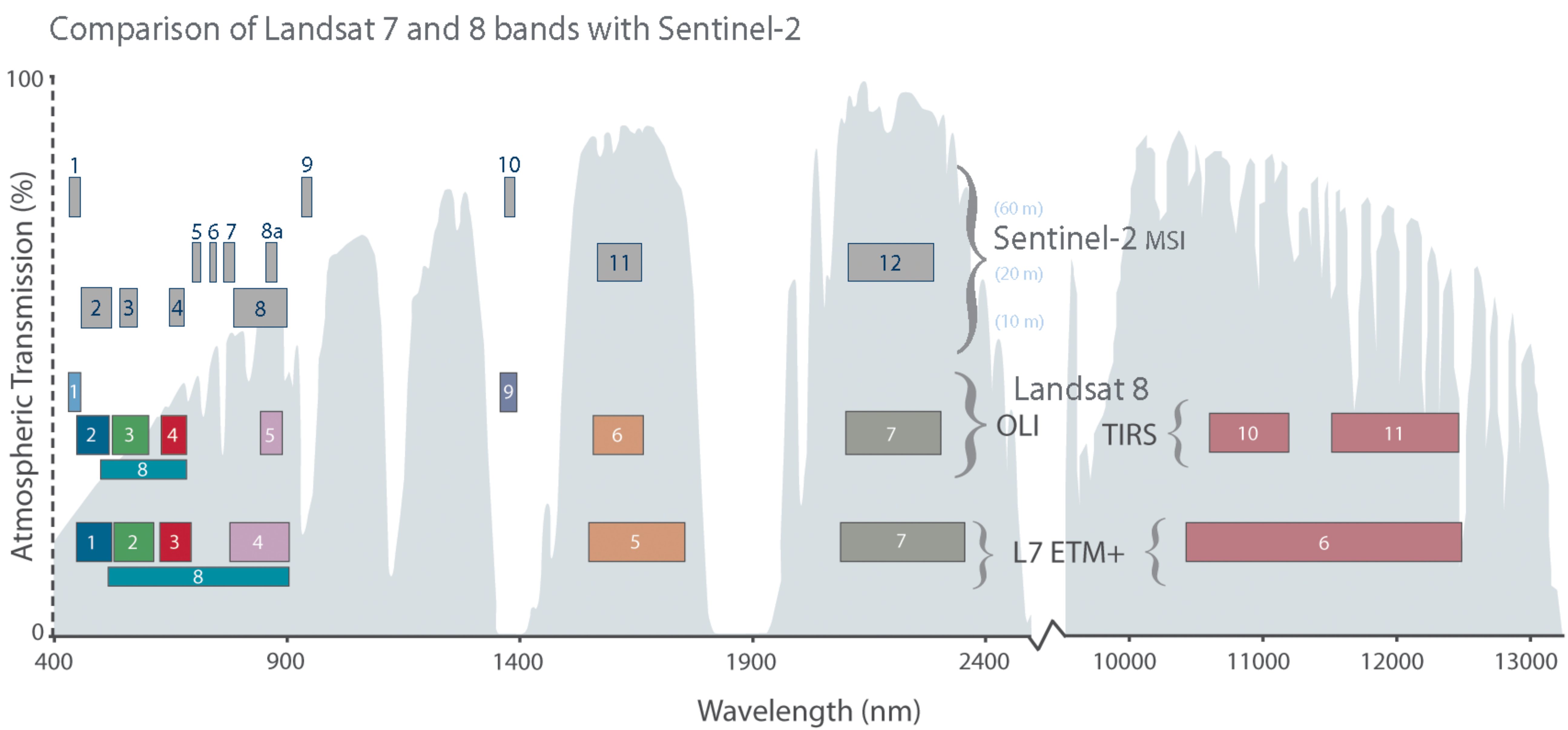

Comparison of Landsat 7 and 8 bands with Sentinel-2
Atmospheric Transmission (%)
100
0
1
9
10
5 6 7
8a
2 3 4 8
11
12
(60 m)
Sentinel-2 MSI
(20 m)
(10 m)
1
9
2 3 4
5
8
6
7
Landsat 8
OLI
TIRS
10
11
1 2 3
4
8
5
7
L7 ETM+
6
400
900
1400
1900
2400
10000
11000
12000
13000
Wavelength (nm)

Source: NASA

Land Monitoring (2017 vs 2018)

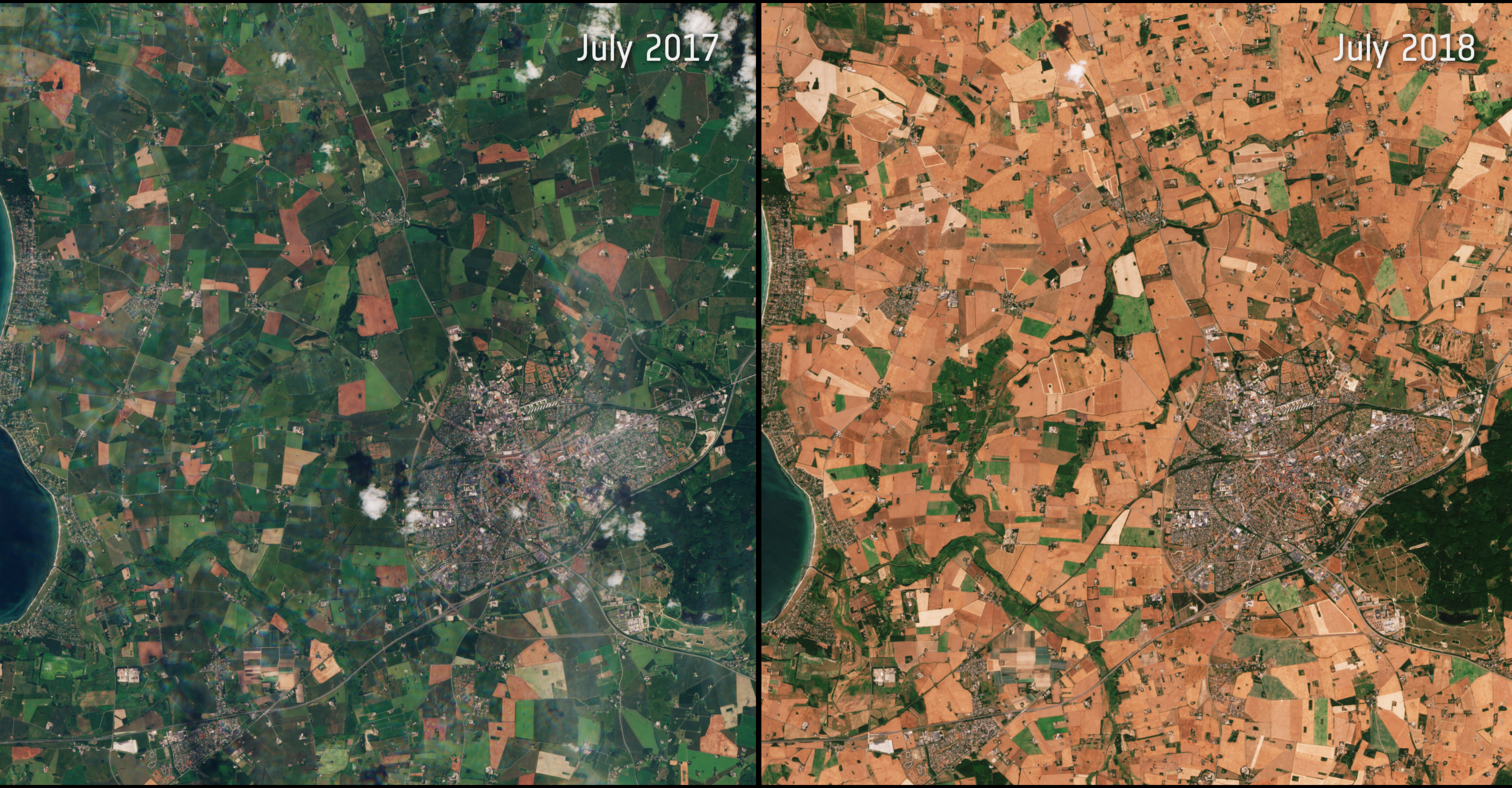

Slagelse in Zealand, Denmark; source: ESA

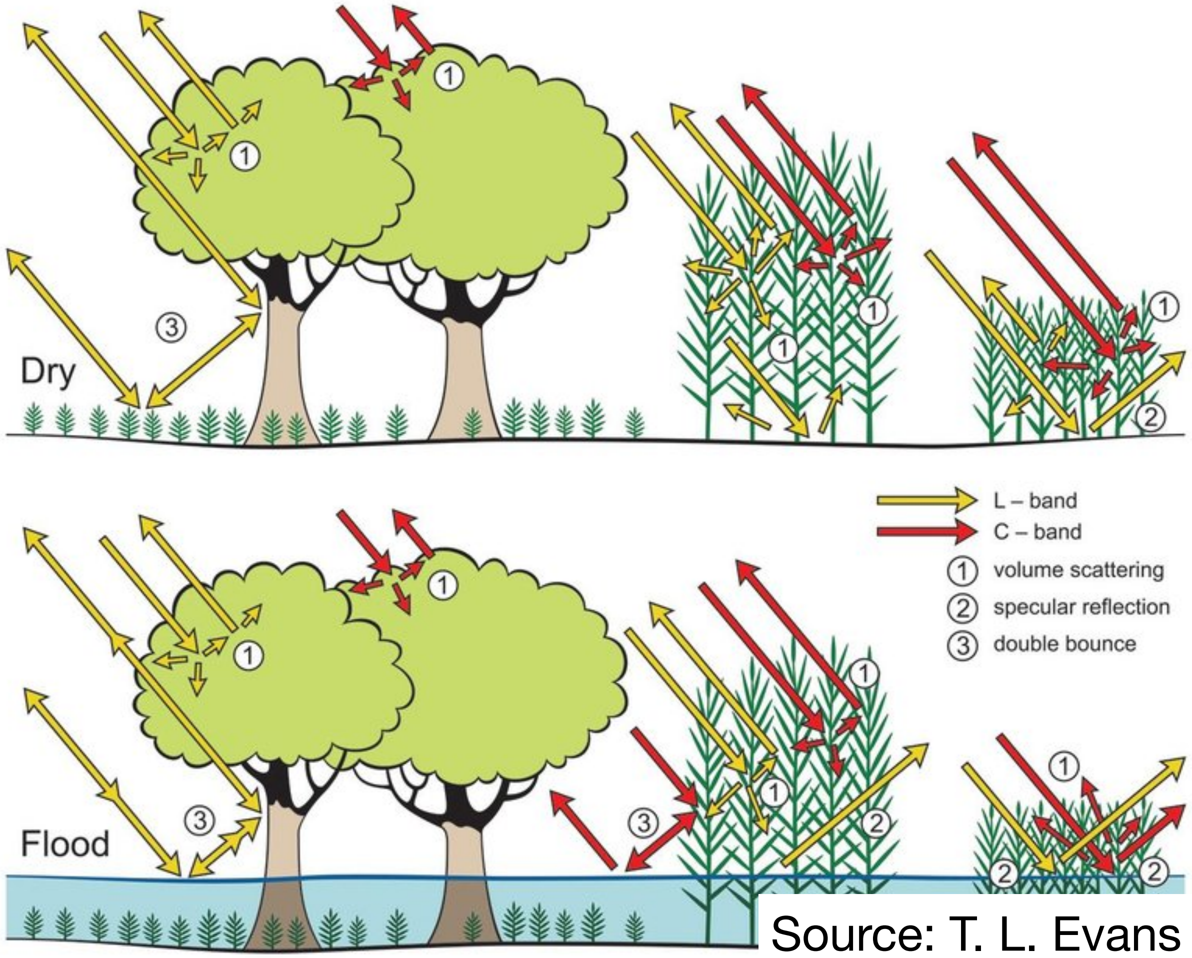

Source: T. L. Evans

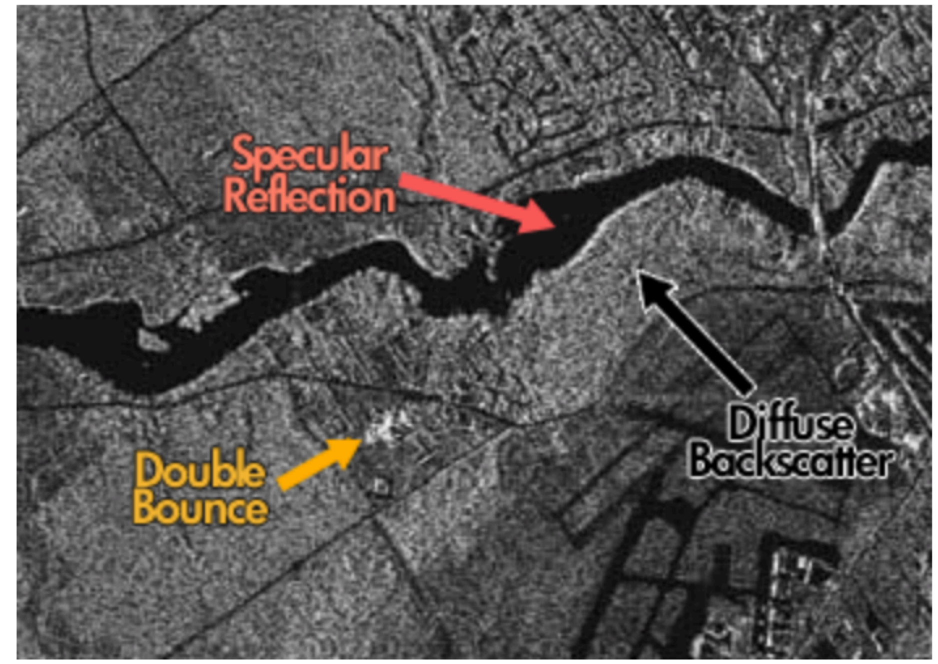

Source: https://gisgeography.com/synthetic-aperture-radar-examples/

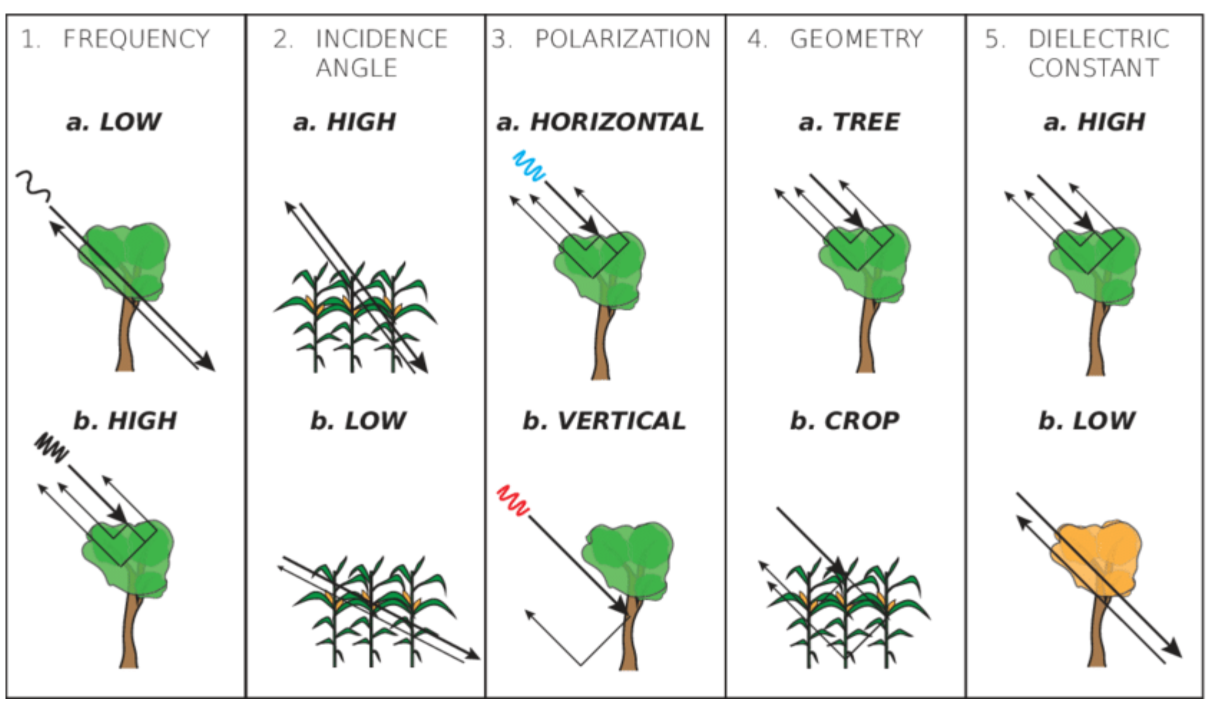

Source: van Emmerik

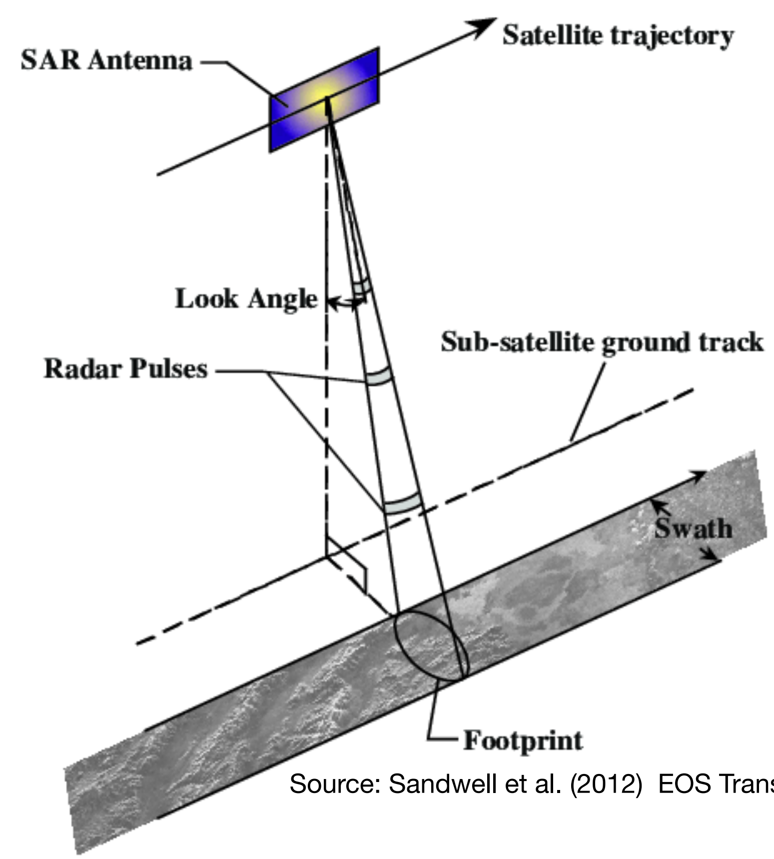

Source: Sandwell et al. (2012) EOS Trans.

Xe-Pian Xe-Namnoy lake (Copernicus Sentinel-1)

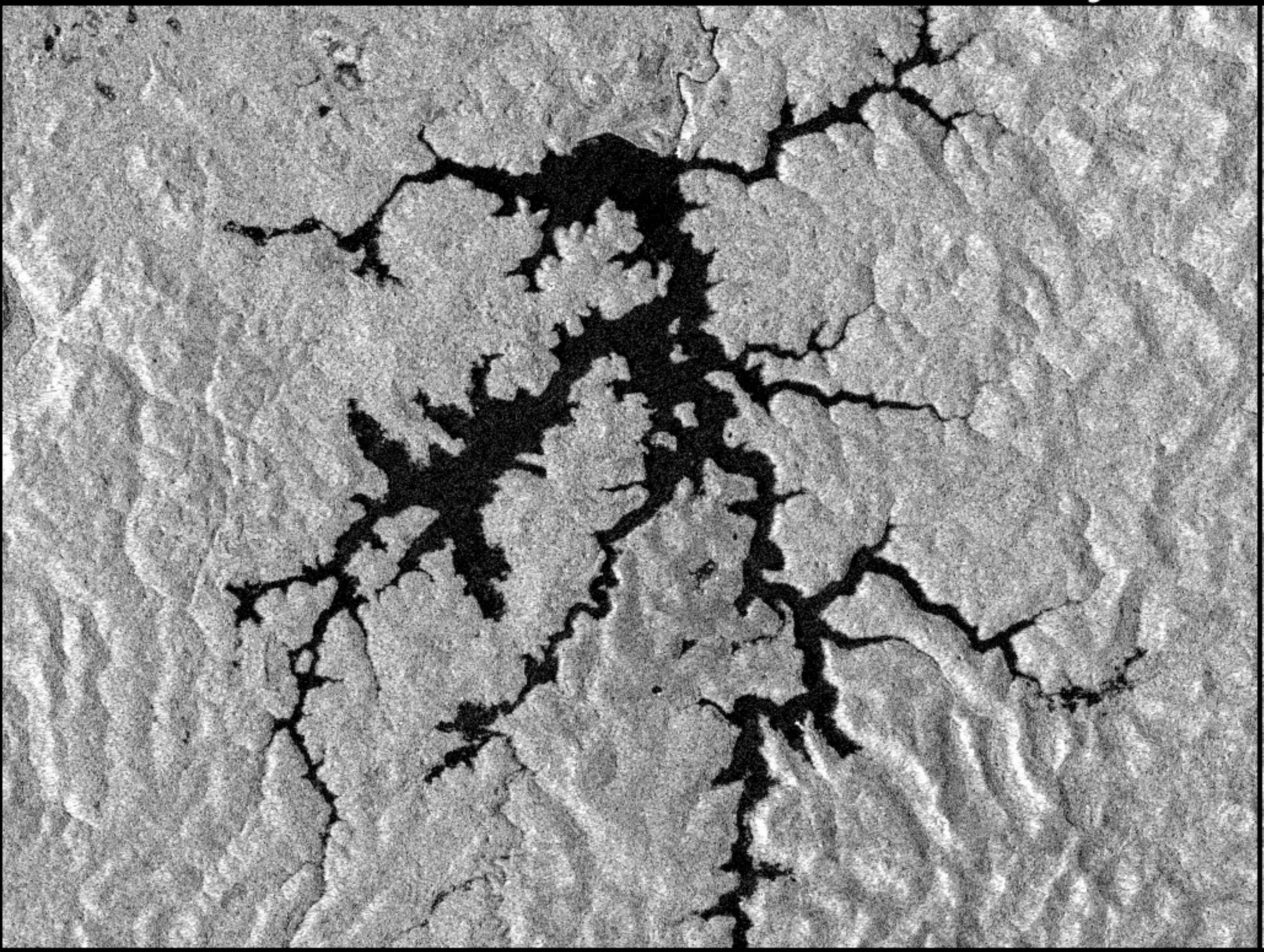

Before dam breach (2018-07-13)

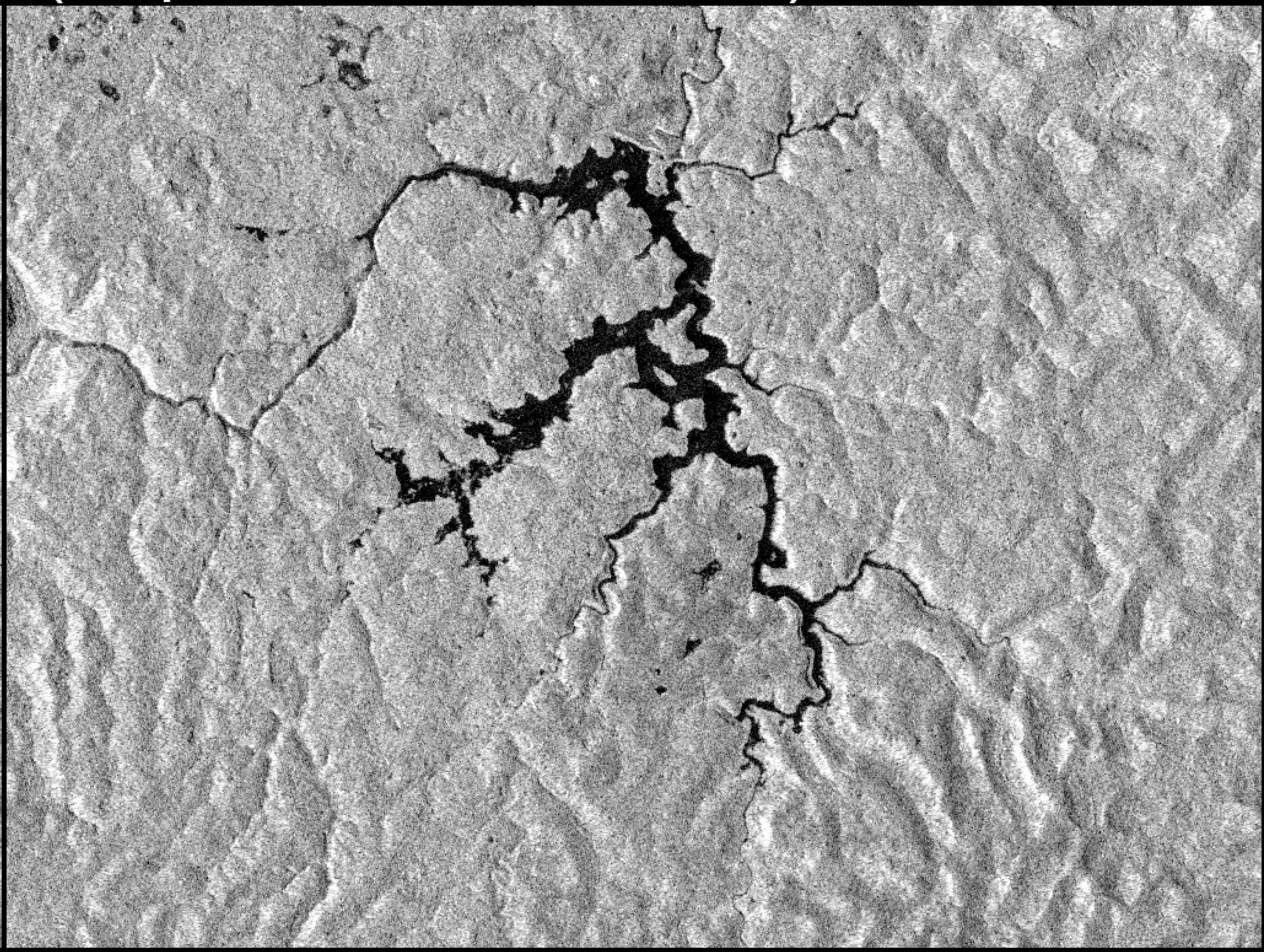

After dam breach (2018-07-25)

Source: ESA / CESBIO

Sentinels Helping to Map Minerals

Sentinel 2

Sentinel 2 (PCA)

SRTM DEM

Geol. Map

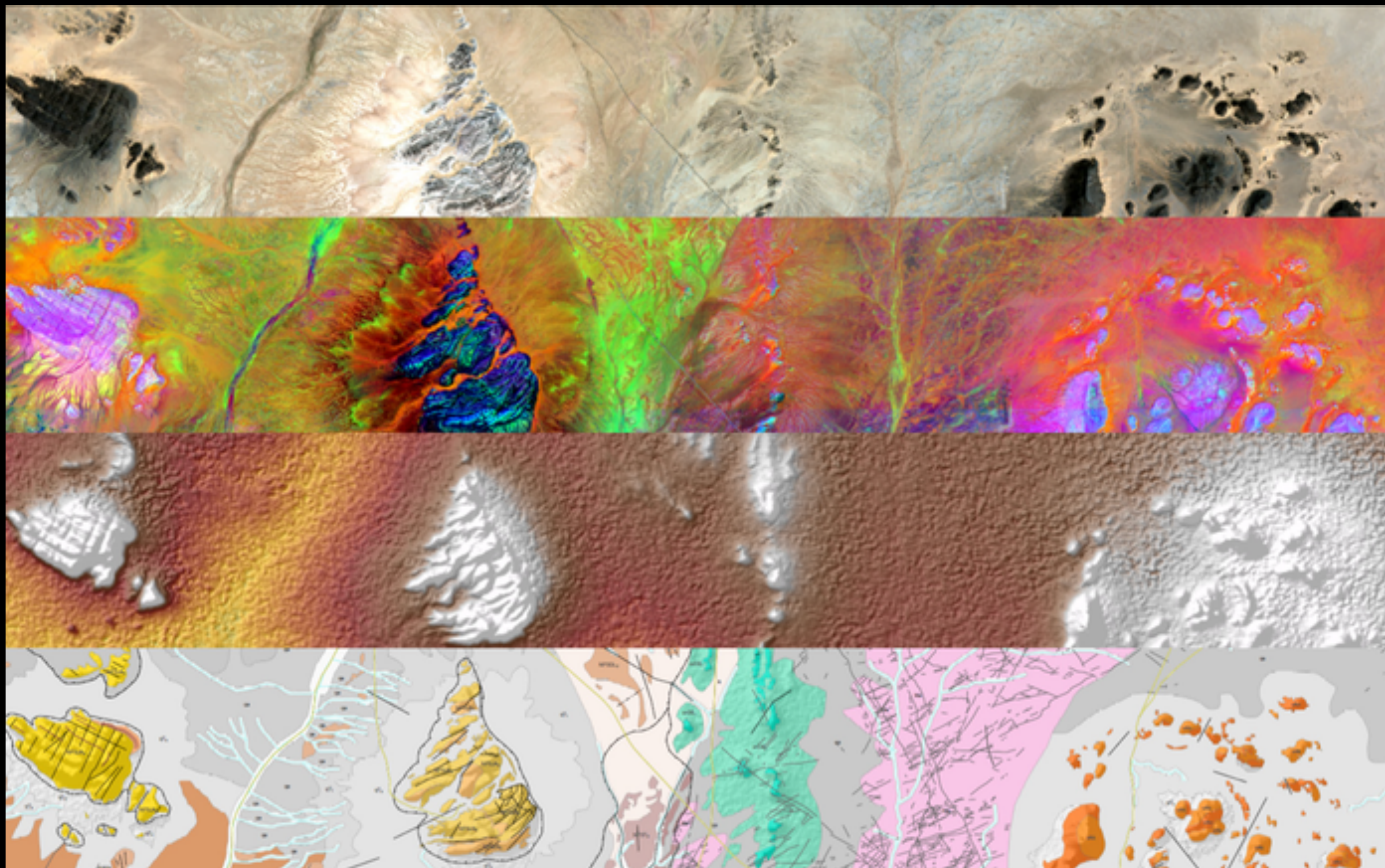

Source: ESA / GAF

Dstl Satellite Imagery Feature Detection

Can you train an eye in the sky?

Featured · 2 years ago · image data, multiclass classification, object segmentation

Planet: Understanding the Amazon from Space

Use satellite data to track the human footprint in the Amazon rainforest

Featured · a year ago · ecology, forestry, image data, object identification

Draper Satellite Image Chronology

Can you put order to space and time?

Featured · 3 years ago · timelines, image data, ranking

Airbus Ship Detection Challenge

Find ships on satellite images as quickly as possible

Featured · 2 months ago · image data, object detection, object segmentation

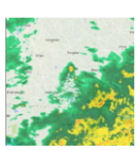

How's the weather?
Predict the amount of rainfall at a location from satellite and numerical weat...
InClass · 4 years ago · Limited

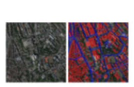

EPFL ML Road Segmentation
Road extraction from satellite images
InClass · 2 years ago · Limited

EPFL ML Road Segmentation
Project 2: Road extraction from satellite images
InClass · a year ago · Limited

ADCG 2016 : Image anomaly detection
Detect cotton crops in a variety of satellite images!
InClass · 2 years ago · Limited

Power up
Classify satellite images of power plants by fuel type
InClass · a year ago · Limited

Here Comes the Sun
Find Solar Panels in Satellite Imagery
InClass · 3 years ago · Limited

Deep Learning Masterclass 1
Classify the orientation of roofs based on satellite images
InClass · 2 years ago · Limited

ADCG SS14 Challenge 03 - Satellite Image Land Patter...
A multi-class classification problem to detect various land pattern via satellit...
InClass · 5 years ago

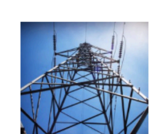

Energy Connections
Identify transmission lines in satellite imagery data
InClass · a month ago · Limited

International Journal of *Geo-Information*

Article

Multi-Temporal Sentinel-1 and -2 Data Fusion for Optical Image Simulation

Wei He and **Naoto Yokoya**

RIKEN Center for Advanced Intelligence Project, RIKEN, Tokyo 103-0027, Japan; wei.he@riken.jp (W.H.); naoto.yokoya@riken.jp (N.Y.)

Received: 26 July 2018; Accepted: 21 September 2018 ; Published: 26 September 2018

Abstract: In this paper, we present the optical image simulation from synthetic aperture radar (SAR) data using deep learning based methods. Two models, i.e., optical image simulation directly from the SAR data and from multi-temporal SAR-optical data, are proposed to testify the possibilities. The deep learning based methods that we chose to achieve the models are a convolutional neural network (CNN) with a residual architecture and a conditional generative adversarial network (cGAN). We validate our models using the Sentinel-1 and -2 datasets. The experiments demonstrate that the model with multi-temporal SAR-optical data can successfully simulate the optical image; meanwhile, the state-of-the-art model with simple SAR data as input failed. The optical image simulation results indicate the possibility of SAR-optical information blending for the subsequent applications such as large-scale cloud removal, and optical data temporal super-resolution. We also investigate the sensitivity of the proposed models against the training samples, and reveal possible future directions.

Keywords: Sentinel; synthetic aperture radar; optical; data simulation; convolutional neural network; generative adversarial network

THE SENTINEL-2 CLOUDLESS LAYER COMBINES OVER 80 TRILLION PIXELS COLLECTED DURING DIFFERING WEATHER CONDITIONS BETWEEN MAY 2016 AND APRIL 2017. IMAGE: ESA.

Aim: Use with high-temp. resolution even if cloudy
Method: Multi-source (S, O) data fusion

Q: Can we use SAR data to predict optical images?

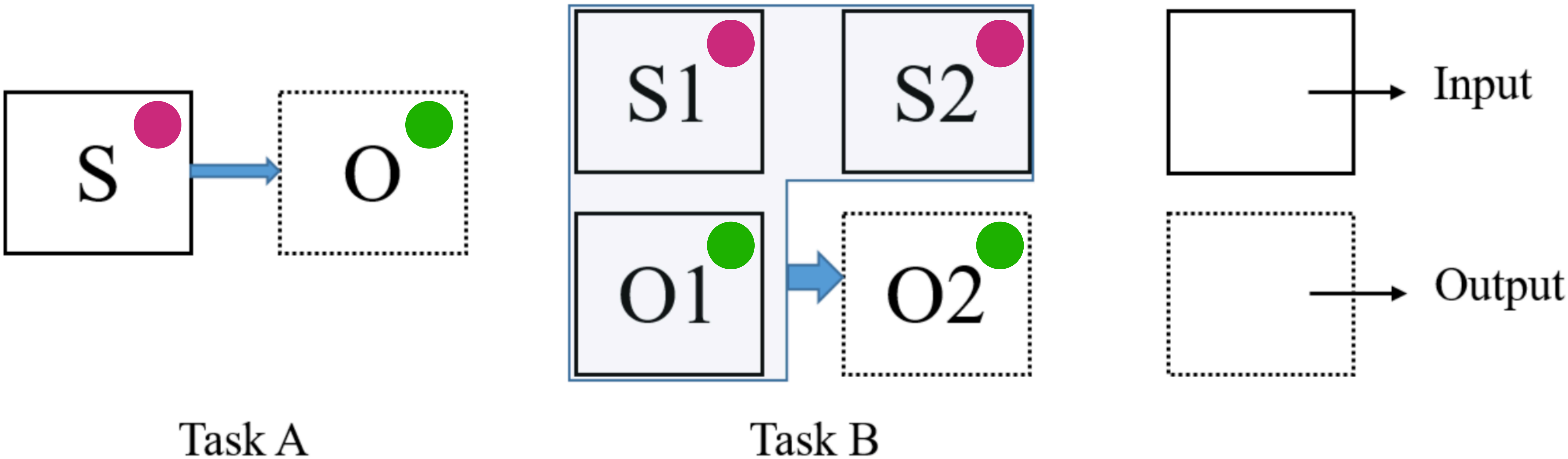

Figure 1. Illustration of two optical simulation tasks.

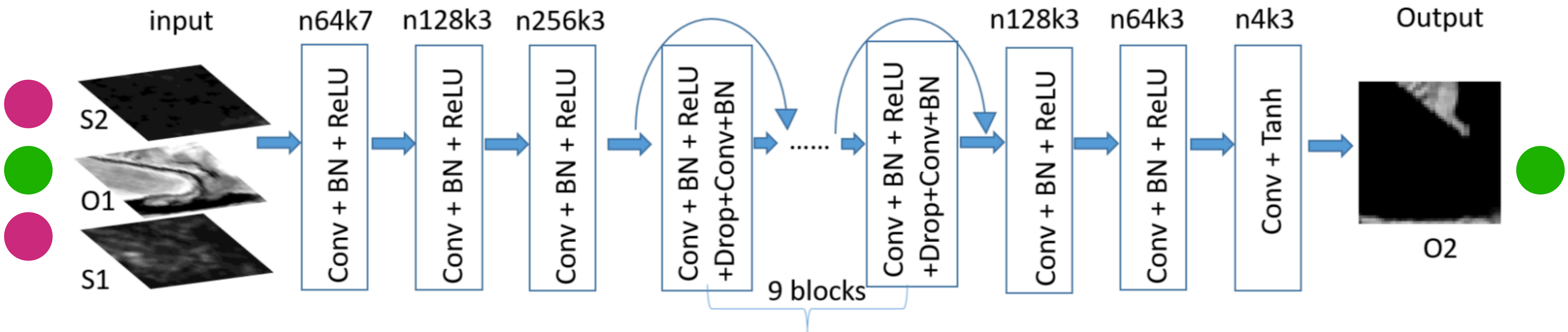

Figure 2. Illustration of the CNN generation network.

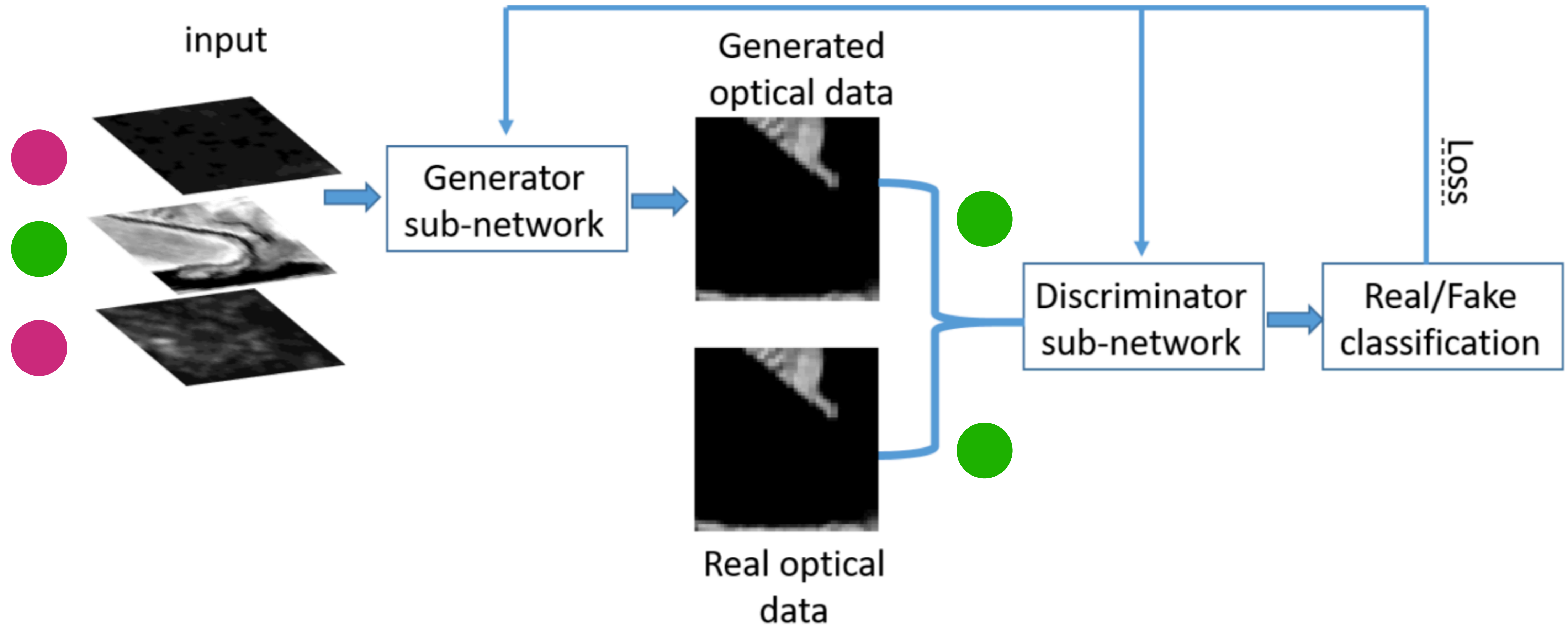

Figure 3. The flowchart of the cGAN architecture.

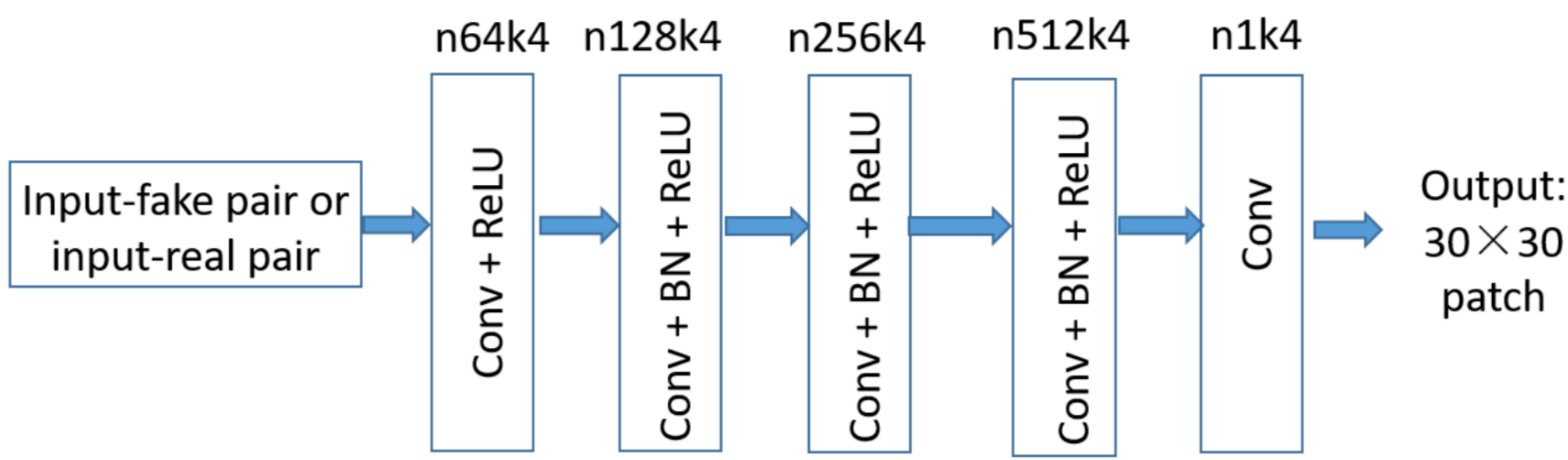

Figure 4. Illustration of the discriminative sub-network.

Fake

? G(x, z)

Discriminator:

y

True

Goal:

D(G(x, z)) = 0

D(x, y) = 1

generative model

discriminative model

cGAN loss:

$$\min_{G} \max_{D} \mathcal{L}_{cGAN}(G, D) = \mathbf{E}_{(x,y) \in p_{data}(x,y)}[logD(x,y)] + \mathbf{E}_{x \in p_{data}(x), z \in p_{data}(z)}[1 - logD(x, G(x,z))]. \quad (1)$$

Reduce blurring with L1 regularization:

$$\mathcal{L}_{L1}(G) = \mathbf{E}_{(x,y) \in p_{data}(x,y), z \in p_{data}(z)} \|y - G(x,z)\|_{L1} \quad (2)$$

Final objective function:

$$G^{*} = \min_{G} \max_{D} \mathcal{L}_{cGAN}(G, D) + \lambda \mathcal{L}_{L1}(G). \quad (3)$$

Table 1. Sensing time of optical and SAR image pairs used in the experiments.

Y-M-D	S1	O1	S2	O2
Iraq	12 November 2017	10 November 2017	6 December 2017	10 December 2017
Jianghan	14 November 2017	12 November 2017	20 December 2017	19 December 2017
Xiangyang	14 November 2017	12 November 2017	20 December 2017	19 December 2017

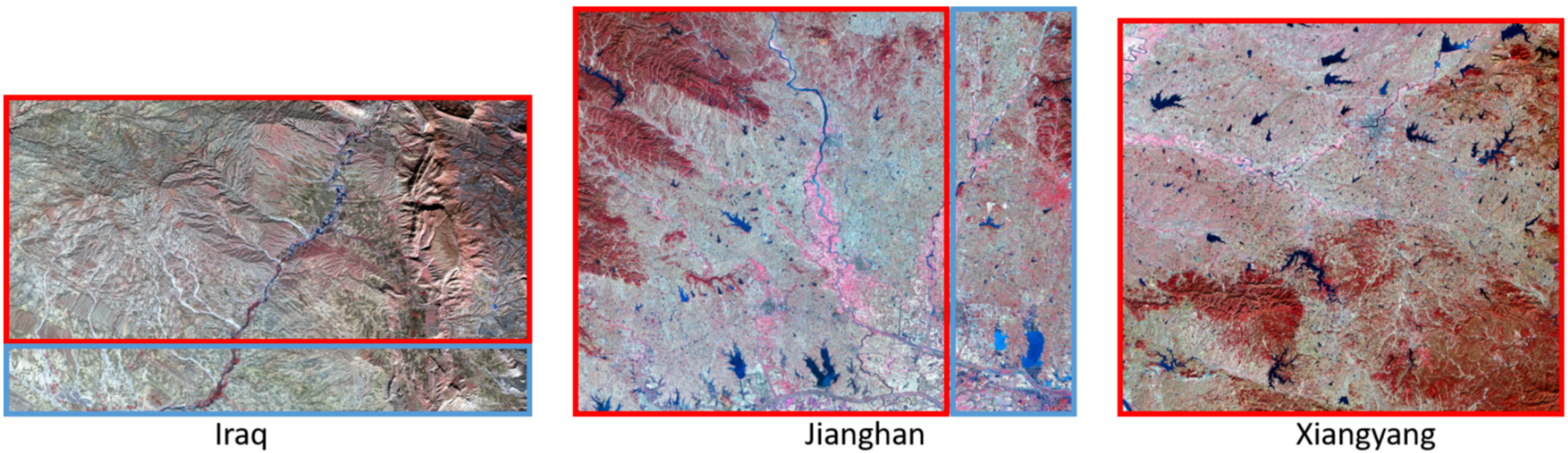

Figure 5. O2 images of Iraq, Jianghan and Xiangyang pairs. The training patches are selected from the red rectangle and the test patches are from the blue area.

Table 2. The training and test Patches provided by the images.

	Iraq	Jianghan	Xiangyang
Train	561	1188	754
Test	99	165	None

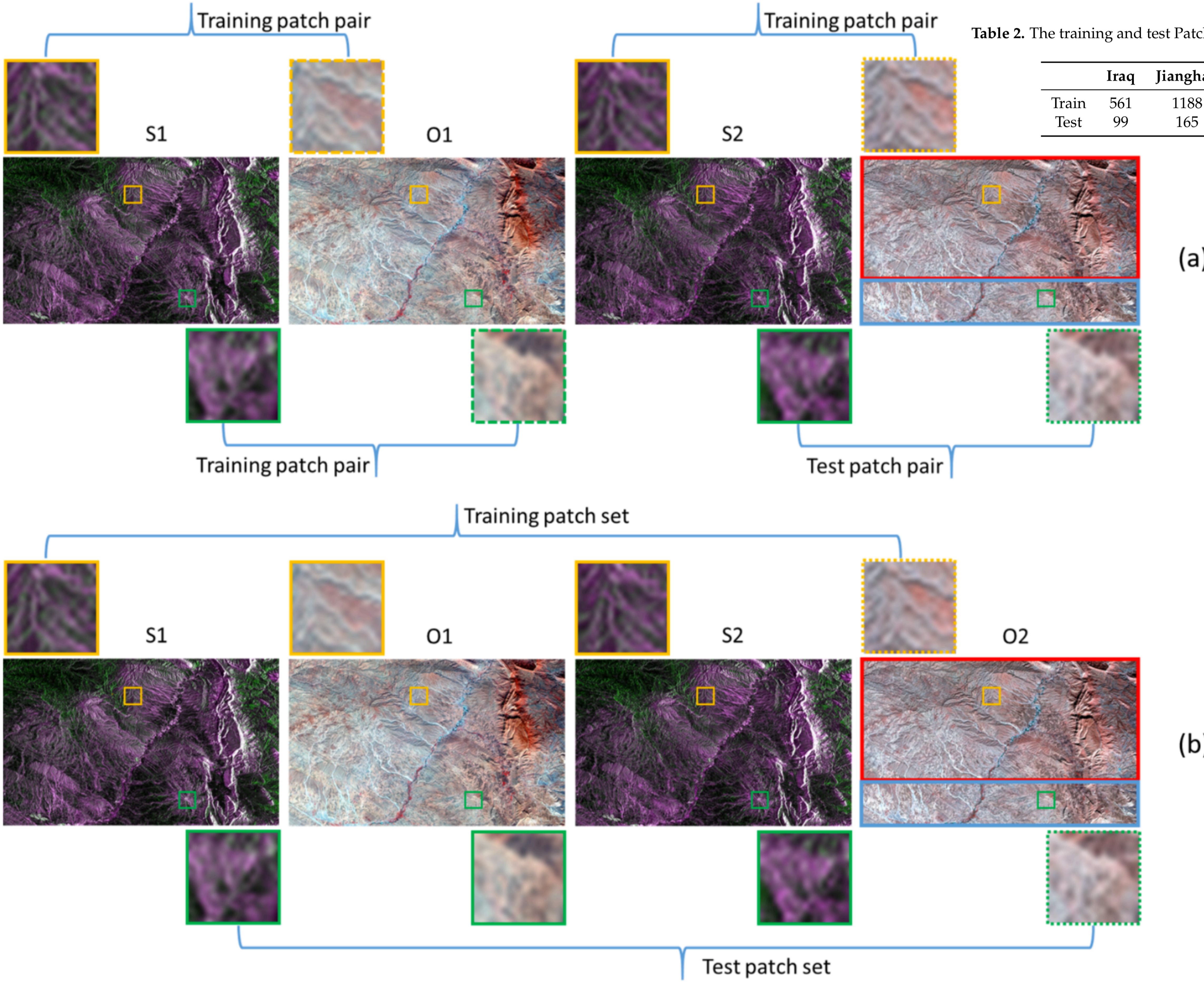

Figure 6. Illustration of training and test patch pairs with Iraq dataset for (**a**) Task A, and (**b**) Task B.

Table 3. The evaluation values of PSNR, SSIM, MSA and training time of different methods in Case 1.

Index	pix2pix	CNN	cGAN	MTCNN	MTcGAN	baseline
PSNR (dB)	26.50	26.60	26.79	30.61	**32.32**	29.77
SSIM	0.6419	0.6477	0.6519	0.9028	**0.9110**	0.8528
MSA	0.6545	0.6769	0.6581	0.3796	**0.3146**	0.5529
Training Time (s)	4252	3747	4025	3506	3892	None

Test patches from Jianghan image (influence of different training sets):

Table 4. Simulation accuracy of MTCNN and MTcGAN with different training samples in Case 2.

Method	Index	Jianghan	Iraq	Xiangyang	Mixed	O1
MTCNN	PSNR	**35.08**	29.44	34.30	34.38	34.01
	SSIM	**0.9508**	0.8585	0.9412	0.9479	0.9401
	MSA	**0.4684**	0.8400	0.5138	0.4774	0.5319
MTcGAN	PSNR	**35.25**	31.09	34.44	34.83	34.01
	SSIM	**0.9509**	0.8850	0.9413	0.9463	0.9401
	MSA	**0.4629**	0.6137	0.5070	0.4649	0.5319

PSNR (peak signal to noise ratio), SSIM (structural similarity), MSA (mean spectral angle)

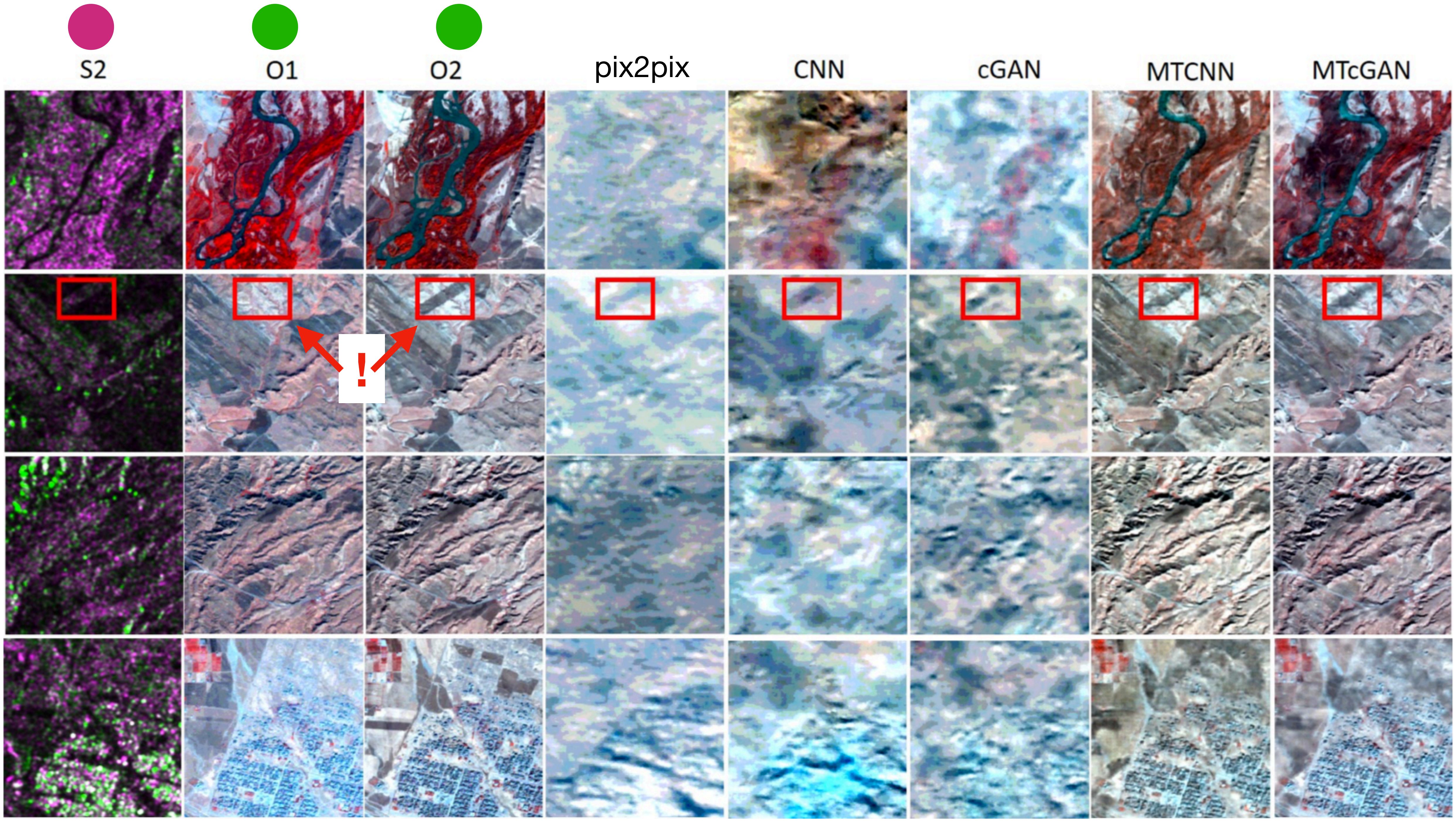

Figure 7. Simulated images of different methods in Case 1, companied with the input images (S2 and O1) and output reference image (O2).

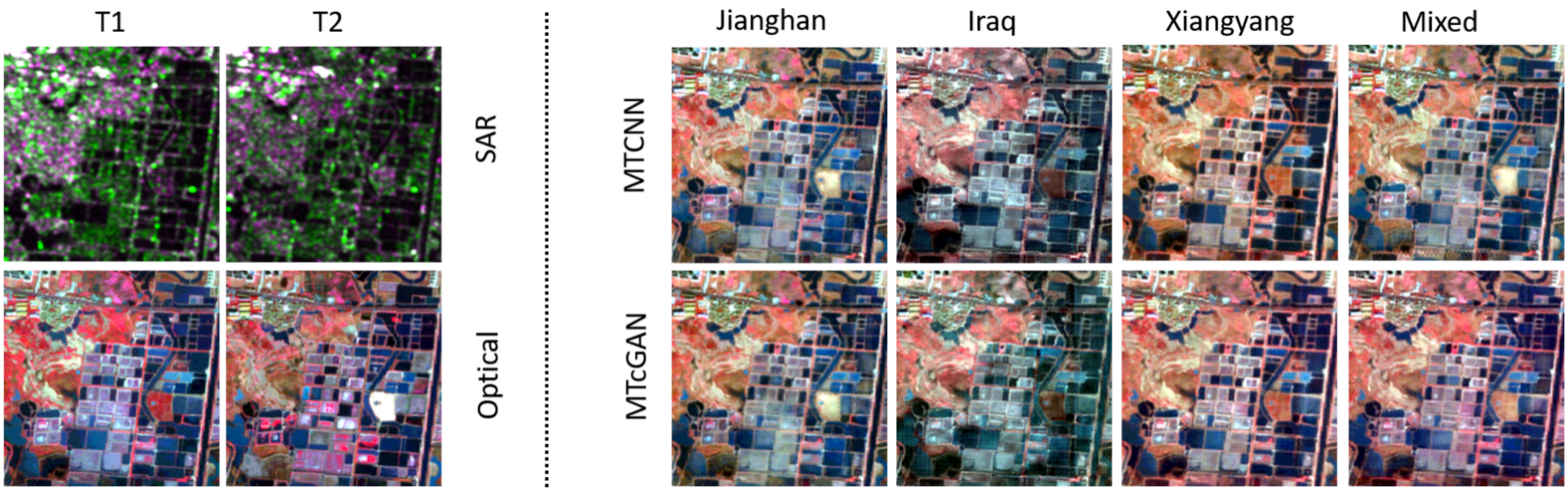

Figure 8. Simulated images of different methods in Case 2. The input images (S1, S2 and O1) and output reference image (O2) on the left side, and simulated images with different training samples on the right side.

Conclusions

- Multi-temporal data fusion based optical image generation works
- Adversarial networks are useful and effective

However:

- Simulated images (O2) in changing parts (S1 -> S2) are blurred
- Selection of training samples has an impact on outcome
- More time-steps could help create more stable results

PSNR is most easily defined via the mean squared error (*MSE*). Given a noise-free $m \times n$ monochrome image I and its noisy approximation K, *MSE* is defined as:

$$MSE = \frac{1}{m\,n}\sum_{i=0}^{m-1}\sum_{j=0}^{n-1}[I(i,j) - K(i,j)]^2$$

The PSNR (in dB) is defined as:

$$\begin{aligned} PSNR &= 10 \cdot \log_{10}\left(\frac{MAX_I^2}{MSE}\right) \\ &= 20 \cdot \log_{10}\left(\frac{MAX_I}{\sqrt{MSE}}\right) \\ &= 20 \cdot \log_{10}(MAX_I) - 10 \cdot \log_{10}(MSE) \end{aligned}$$

PSNR: peak signal to noise ratio

Here, MAX_I is the maximum possible pixel value of the image. When the pixels are represented using 8 bits per sample, this is 255. More generally, when samples are represented using linear PCM with B bits per sample, MAX_I is $2^B - 1$.

The SSIM index is calculated on various windows of an image. The measure between two windows x and y of common size $N \times N$ is:[4]

$$\mathrm{SSIM}(x,y) = \frac{(2\mu_x\mu_y + c_1)(2\sigma_{xy} + c_2)}{(\mu_x^2 + \mu_y^2 + c_1)(\sigma_x^2 + \sigma_y^2 + c_2)}$$

with:

- μ_x the average of x;
- μ_y the average of y;
- σ_x^2 the variance of x;
- σ_y^2 the variance of y;
- σ_{xy} the covariance of x and y;
- $c_1 = (k_1 L)^2$, $c_2 = (k_2 L)^2$ two variables to stabilize the division with weak denominator;
- L the dynamic range of the pixel-values (typically this is $2^{\#bits\ per\ pixel} - 1$);
- $k_1 = 0.01$ and $k_2 = 0.03$ by default.

SSIM: structural similarity

Source: Wikipedia

MSA: mean spectral angle

$$\mathrm{MSA} = \frac{180}{\pi} \frac{\left(\sum_{\mathrm{i}=1}^{\mathrm{N}} \arccos\left(\sum_{\mathrm{v}=1}^{\mathrm{M}} Z^{*}(x_i, t, v) Z(x_i, t, v) \Big/ \sqrt{\sum_{\mathrm{v}=1}^{\mathrm{M}} Z^{*2}(x_i, t, v) \sum_{\mathrm{v}=1}^{\mathrm{M}} Z^{2}(x_{\mathrm{i}}, t, v)} \right) \right)}{N},$$

Source: Yin et al., 2017, Int J Rem Sens